Glass Fiber Poling and Applications

Peter G. Kazansky, Philip St. J. Russell, and Hiromichi Takebe

(Invited Paper)

***Abstract*— Recent developments in the application of poled optical fibers to second harmonic generation and electrooptic light modulation are reviewed.**

***Index Terms*— Electrooptic switches, glass materials/devices, integrated optics, optical fiber devices, optical frequency conversion, nonlinear optics.**

I. Introduction

SILICA glass is a dominant material in optoelectronics largely because of its low fabrication cost compared to crystalline materials, and its superior optical properties such as high transparency and high optical damage threshold. Its position has recently been enhanced by the discovery that exposure to UV light causes permanent changes in refractive index at communications wavelengths. This effect, which requires the presence of dopants such as Ge or Ce, has made possible the routine fabrication of important passive components such as Bragg grating filters and mirrors. More recently, a variety of different poling techniques have proved unexpectedly effective in producing substantial second order nonlinearities—the subject of this article. These developments are likely to lead to glass fibers with built-in functions such as linear electrooptic modulation and switching, and parametric frequency conversion.

The first reports of second-harmonic (SH) generation in silica fibers date back to the late 1980's, when it was discovered that prolonged exposure to infrared light causes the self-organized growth of green SH light [1]. Wide-ranging studies ensued into the mechanism and properties of this unexpected photoinduced phenomenon [2]–[17]. Its mystery was finally attributed to the coherent photo-galvanic effect [5], [6] in which a high (10^4–10^5 V/cm) dc electrostatic field appears as a result of the charge separation induced by the coherent photocurrent, oscillating spatially with a period determined by the coherence length. This produces a quasi-phase-matching $\chi^{(2)}$ grating in proportion to the product of the electric field and $\chi^{(3)}$. This phenomenon proved of more scientific than practical interest, owing to levels of nonlinearity that are typically three to four orders of magnitude less than in the best nonlinear crystals.

Since 1991, however, second-order nonlinearities of order 1 pm/V have been achieved in glasses using a variety of different techniques: thermal poling [18], corona poling [19], electron implantation [20]. Most recently, an electrooptic coefficient of ~6 pm/V has been reported in a specially fabricated side-hole fiber after UV-excited poling [41]. These observations have excited considerable interest because they suggest that efficient all-glass linear electrooptic modulators and frequency convertors are imminent [21]–[48]. Considering that interaction lengths tens of cm long are feasible in optical fiber (compared to few cm in ferroelectric crystals), even nonlinearities of ~1 pm/V place silica glass in the position of a serious potential rival to important crystals such as lithium niobate, potassium titanyl phosphate (KTP) and lithium triborate (LBO).

Although to date the nonlinearity produced by the thermal poling technique appears to be the most reliable and stable (although very long term studies are yet to be carried out, shows no degradation under illumination with intense visible and infrared light), its origin is not still fully understood. Two mechanisms have been proposed. One involves the orientation of bonds or dipoles [24] and the other a frozen-in electric space-charge field [18], [31]. Despite the fact that a frozen-in field is more likely to be responsible, none of this two mechanisms have yet obtained full confirmation [31], [44]. Both predict the second-order nonlinearity to depend on the strength of the electrical field in a depletion region that forms near the anodic surface.

Electrooptic phase modulation has been demonstrated in a thermally poled fused silica channel waveguide made by electron implantation [23], and an electrooptic coefficient of about 0.3 pm/V has been measured in thermally poled silica glass [27]. Most recently electrooptic switch has been demonstrated in a poled silica-based waveguide on Si substrate [43]. Quasi-phase-matched frequency doubling of Q-switched Nd:YAG laser light at 1064 nm has been demonstrated in thermally poled silica glass [30]. The nonlinear coefficients are still small and so require long interaction lengths. This is not a significant problem in fiber-based devices which anyway guarantee low cost, integrability and easy packaging. In addition, the use of poled fibers would simplify optoelectronic systems and reduce the insertion loss and packaging costs associated with coupling of discrete optical components.

In the remainder of this paper, we review, in the context of the work of other groups, our recent progress on second

Manuscript received February 24, 1997.

P. G. Kazansky is with the Optoelectronics Research Centre, University of Southampton, Southampton SO17 1BJ, UK.

P. St. J. Russell is with the Optoelectronics Group, School of Physics, University of Bath, Claverton Down, Bath BA2 7AY, UK.

H. Takebe is with the Department of Materials Science and Technology, Graduate School of Engineering Sciences, Kyushu University, Fukuoka 816, Japan.

Publisher Item Identifier S 0733-8724(97)05946-X.

TABLE I
SUMMARY OF FIBER PREFORMS TESTED BY THERMAL POLING. EFNQ = ELECTRICALLY FUSED NATURAL QUARTZ; FFNQ = FLAME FUSED NATURAL QUARTZ

Preform (type)	*Glass tube*			*Inner cladding*	*Core*
	Type	*Name*	*OH* (ppm)		
A (MCVD)	EFNQ	GE-100	~1	P+F doped silica	3.5 mol% GeO_2
B (MCVD)	FFNQ	Herasil 1	~150	P+F doped silica	18 mol% GeO_2 + Na
C (MCVD)	FFNQ	Herasil 1	~150	–	3.9 mol% GeO_2
D (MCVD)	FFNQ	Herasil 1	~150	–	4.5 mol% GeO_2 + Na
E (VAD)	–	–	~40	–	8 mol% GeO_2

harmonic generation and electrooptic light modulation in poled optical fibers [47], [48].

II. POLING OF FIBER PREFORMS

In our first experiments, fiber preforms with different compositions were thermally poled to identify the best core and cladding compositions and to understand better the underlying mechanism [25]. The preforms investigated are listed in Table I. Slices approximately 1 mm thick from each preform were thermally poled at 2.5 kV applied voltage and 280 °C temperature for 15 min in an oven. Stainless steel and silicon electrodes were used.

After poling, the electrodes were removed and the samples tested for evidence of second harmonic generation (SHG). *Q*-switched and mode-locked Nd:YAG laser operating at 1064 nm was used as a pump source. The laser beam was focused to a spot size of ~50 μm (using a lens with focal length 10 cm) on to the anodic surface. The angle of incidence (~60°) was chosen to lie close to the Brewster angle. After crossing the sample, the diverging laser radiation was focused with a second lens on to separate detectors for pump and second harmonic light. The second harmonic signal was monitored while translating the sample in a direction perpendicular to the plane of incidence. There was not any SH signal detected in any region of preforms A and E. In contrast, a strong SH signal was observed in the starting tube in preforms B, C, and D, and no SH signal was observed in the P + F-doped cladding while scanning along preform B with a *p*-polarized pump (see Fig. 1). A small peak in SH signal was also observed at the boundary between the starting tube and the cladding with *s*-polarized pumping. This may be explained by the existence of a fringing (nonnormal) electrostatic field at the boundary between the two regions. This has been confirmed by the observation of a peak in the SH signal at the boundary while scanning the pump beam (at normal incidence) along the surface of the sample. We observed ~15% stronger SH signal in the Ge-doped core compared to the starting tube (see Fig. 2). The SH signal in the core was also found to follow the Ge concentration. The measured absorption spectrum in the core region of preforms C and D indicated an OH concentration of ~80 ppm.

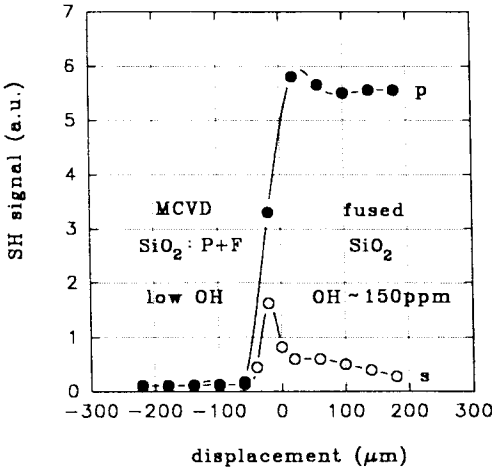

Fig. 1. SH signals for *p*-polarized pump (•) and *s*-polarized pump (o) in the cladding and starting tube in preform B.

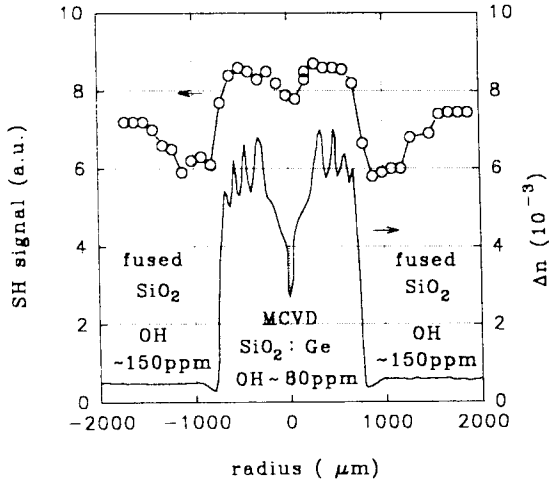

Fig. 2. SH signal (o) and refractive index difference in preform C.

Our results may be explained by a high Na^+ or H^+ content in the starting tubes and preform core where they act as positively charged carriers; interestingly, sodium doping ($\leq$10 ppm preform D) produced no significant effect on the SH signal. However, the latter result can be explained by a saturation of the SON even at small (<1 ppm) concentrations of Na impurities whaich are always present in fused quartz.

III. POLING OF SILICA FIBERS

For the fiber poling experiments, preform B and a preform similar to preform C (GeO_2 concentration about 1.5 times less then in preform C) were pulled into fiber B (core diameter 2 μm, outer diameter 100 μm, numerical aperture 0.27) and fiber C (core diameter 16 μm, outer diameter 125 μm, numerical aperture 0.09), respectively [25]. The OH concentrations were 80 and 150 ppm, respectively, in the core and in the cladding (formed from Herasil-1). Regions ~8 mm long were side-polished to within about 1 μm of the core. The side-polished fibers were placed on top of a 2-mm-thick silica substrate manufactured by the same method as the starting tubes (Herasil-1), and the final assembly was sandwiched between two electrodes with the anodic electrode on top of

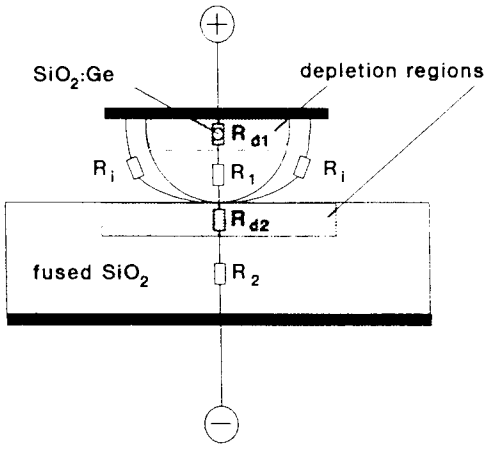

Fig. 3. Diagram of the fiber thermal poling arrangement and corresponding equivalent circuit.

the polished fiber surface (see Fig. 3). Thermal poling was carried out at 4.3 kV and 280 °C for 15 min.

After thermal poling, pump light was launched into the fibers. No SH signal was seen in fiber B. In contrast, a strong nonphase-matched SH signal (visible to the naked eye) was observed in fiber C. We obtained a conversion efficiency $3 \times 10^{-6}\%$ at an infrared pump power of ~1 kW. Taking into account the fact that the SH signal in a nonphase-matched geometry is generated over the coherence length ($\Lambda_{coh} = \lambda/[4(n^*_{2\omega} - n^*_{\omega})] \simeq 20$ μm where $\lambda = 1064$ nm, $n^*_{2\omega}$ and n^*_{ω} are the effective indices of the SH and infrared fiber modes), the effective value of the induced second-order susceptibility [$\chi^{(2)}_{\text{eff}} = \chi^{(2)}\eta$ where η is the overlap integral between the nonlinearity and the modal field] was estimated to be about 0.2 pm/V. Because the fiber geometry is more complicated, exact measurements of the thickness and location of the nonlinear layer are difficult. Nevertheless, assuming the thickness of the nonlinear layer to be about 7 μm [22] the value of overlap factor for our fiber is $\eta \leq 0.4$, which yields the value of $\chi^{(2)} \geq 0.5$ pm/V.

Experiments on electron beam poling were also carried out in side-polished Ge-doped fiber (core diameter 4 μm, outer diameter 90 μm, numerical aperture 0.3) with 22.7 mol% GeO_2. Fiber samples were irradiated in a scanning electron microscope (SEM) at 0.3 nA beam current and 40 kV beam voltage. The TV mode of a SEM (horizontal scanning rate 0.064 ms/line, vertical scanning rate 20 s/frame) was used. Areas of about 0.01 mm^2 on the surfaces of fiber samples were irradiated for 1 min. After irradiation, the fibers were tested for evidence of SHG. Values of $\chi^{(2)}_{\text{eff}} \simeq 0.1$ pm/V were obtained in the fibers. The result obtained using electron beam poling of Ge-doped silica are perhaps explained by Ge-related defect centres, which act as traps for implanted electrons and also may cause an increase in secondary electron emission which finally leads to the production of a dipole layer of both positive and negative charge.

In our fiber poling experiments, we noticed that the reproducibility of the second-order nonlinearity is rather low—only of about 3% of poled fibers had a $\chi^{(2)}$ of ~0.2 pm/V—most had a nonlinearity an order of magnitude lower. Such poor reproducibility can be explained by electrical breakdown in the air [26]. Indeed, we discovered that the supporting silica substrate (underneath the fiber) was also poled (Fig. 3), despite there being no direct electrical contact.

To avoid air breakdown, we poled fibers in an evacuated chamber and achieved improved reproducibility. We used fiber C in these experiments. Thermal poling was carried out in an evacuated chamber at $\sim 1.2 \times 10^{-5}$ mbar. Poling assembly and parameters were the same as for poling in air. Second harmonic tests of the vacuum poled fibers showed almost 100% reproducibility of the value of effective second-order susceptibility $\chi^{(2)}_{\text{eff}}$ of about 0.2 pm/V [$\chi^{(2)}_{\text{eff}} = \chi^{(2)}\eta$ where η is the overlap factor between fiber mode and the nonlinearity]. The use of some high dielectric strength polymer [29], gas, or oil can also help to solve the problem of breakdown.

IV. Effect of Poling Conditions on SHG in Fused Silica

The effective second-order nonlinearities are still small. Considerable improvements may be expected by optimizing of poling conditions, e.g., the poling time and the applied dc voltage. If we assume the following:

a) that the induced $\chi^{(2)}$ is proportional to the electric field and the pump propagates transversely to the poled region of the bulk sample;
b) that the poling process has reached equilibrium (i.e., the entire applied voltage is taken up across the depletion layer);
c) that the poled layer is significantly less than a Maker fringe thick (phase matching preserved throughout the layer);

then the SH signal will be proportional to the applied voltage squared (i.e., the square of the line integral of electric field across the poled layer). A close to quadratic dependence of the SH signal on voltage has been observed in poled SiO_2 thin films on Si [32]. Other reports suggest a dependence of SH signal on the *third* power of the applied voltage in bulk fused silica samples [18]. Neither proposed mechanisms of glass poling (dipole orientation and frozen-in electric field) explain the latter result. The dependence of second-order nonlinearity on poling time (which may give important information about poling mechanism) is also not fully investigated. Indeed, *in situ* measurements of SH signal during poling (with applied voltage switched-on continuously during poling) show very rapid rise times of SH signal of about several seconds [24]. However, measurements of the SH signal *after poling* (no systematic measurements of such dependences have been carried out so far) show that it takes an order of tens of minutes for the SH signal to saturate.

We carried out experiments to clarify the influence of poling conditions, in particular poling voltage and poling time, SHG in thermally poled silica glass [47]. Herasil 1 samples were used in the experiments. Q-switched and mode-locked Nd:YAG laser pulses at 1064 nm (average power 850 mW) were used as a pump source. We examined the effect of poling conditions on SH generation in fused-silica samples poled both in air and in evacuated chamber. The samples as received were 3-mm-thick (new) Herasil-1 and were poled at 280 °C. After

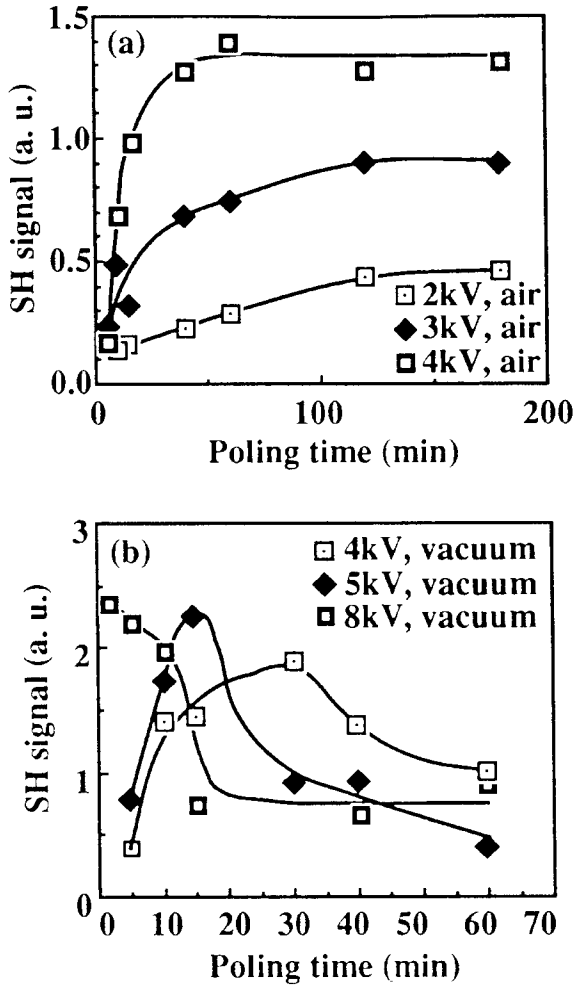

Fig. 4. SH signal versus poling time (a) in air and (b) in vacuum for the 1-mm-thick, as-received Herasil-1 samples. SH signals are normalized to the SH signal in a reference sample poled at 280 °C and 4 kV for 15 min in air.

an appropriate time, samples were subsequently taken from the oven and cooled to room temperature with the field applied. The cooling times from 280 to 200 °C were 9 and 1 min in the chamber and in air, respectively.

The results show that the SHG signal in air-poled samples increases exponentially with the poling time up to a saturation level [Fig. 4(a)]. The growth rate clearly depends on the applied voltage. The times $t_{1/2}$ taken for the amplitude of the SH signal to reach its half-maximum level ($t_{1/2} = \tau \ln 2$ were τ is the relaxation time) were 6.5, 7.8, and 11 min for applied voltages of 4, 3, and 2 kV. This shows that there is an approximately inverse linear dependence of the time constant τ on the applied voltage in the measured range. Assuming that the poling phenomenon is caused by frozen-in electrical field, we note that the Maxwell relaxation time is $\tau = \varepsilon\varepsilon_0/\sigma$, where σ is the conductivity in the depletion region. This dependence of the relaxation time on the applied voltage reveals that the conductivity inside the depletion region increases with the applied voltage.

Results previously obtained from *in situ* measurements of the SH signal (with applied voltage switched-on continuously), in particular very fast rise times (several seconds) and the independence of this rise time of the applied voltage, seem to contradict the above results [23]. This contradiction may, however, be resolved if the poling process takes place in two stages.

During the first stage, cations such as Na^+, H^+, or holes move to the cathode, leaving behind a negatively charged depletion region. A very high electric field arises in this region, between the negatively charged region and the anode, peaking at the glass/anode interface. This field creates a second-order nonlinearity [$\chi^{(2)} = 3\chi^{(3)}$ E] and a corresponding SH signal that is detected during *in situ* measurements. After cooling and removal of the anode, this nonlinearity will not be stable since the sample is negatively charged. Positive charge will be attracted to it, thereby, shifting the position of zero electric field toward to middle of the depletion region. This will greatly reduce the SH signal. During the poling step, the speed of the formation of the depletion region—several seconds—is determined by the cationic conductivity of the glass, which is relatively high at an elevated temperature of about 280 °C. Cationic conductivity takes place in the whole volume of the glass, where the strength of the electrical field is much lower than in the depletion region, which explains why this conductivity (rise time) is independent of the applied voltage.

During the second stage of the poling process, some process akin to avalanche multiplication takes place in the very high electric field at the anode/glass interface. This will cause removal of negative charge from the depletion layer. Electrons are likely to be the predominant charge carriers in this region. After completion of this breakdown process, a permanent dipole field will appear near the anodic surface between layers of positive and negative space charge, thus, creating a stable second-order nonlinearity. The conductivity in the depletion region will depend on the applied voltage because of the very high electric field strength (more than 10^7 V/cm) in this region. Indeed, the results of our experiment may be interpreted as an indication that the conductivity inside the depletion increases with the electrical field strength (applied voltage). Laser-induced pressure pulse probing of the charge distribution is in a very good agreement with this model [44].

Because of electrical breakdown in the air, it was impossible to apply voltages higher than 4 kV to the silica samples in air. In vacuum poled samples, SH signal shows a maximum for each dc voltage and this maximum shifts to a shorter poling time with increasing applied dc voltage [Fig. 4(b)].

The dependence of SH signal on dc voltage for the as-received samples reveals that the SH signal is proportional to the square of the applied dc voltage (Fig. 5). Note that the samples were poled at 280 °C for the optimum time needed to create the maximum SH signal for each dc voltage applied (see Fig. 4) and that line (a) in Fig. 5 was fitted only to samples poled in air. Saturation of the SH signal is observed at dc voltages as high as 8 kV, in good agreement with the results of previous measurements [18].

To examine the annealing effect on SHG in fused silica, we used samples that were poled and annealed repeatedly. Sample annealing before poling was performed at 350 °C for more than 1 h. The SH signal in these samples was already saturated after 5 min of poling at 280 °C and 4 kV (see Fig. 6) [in experiments with fresh as-received samples it takes

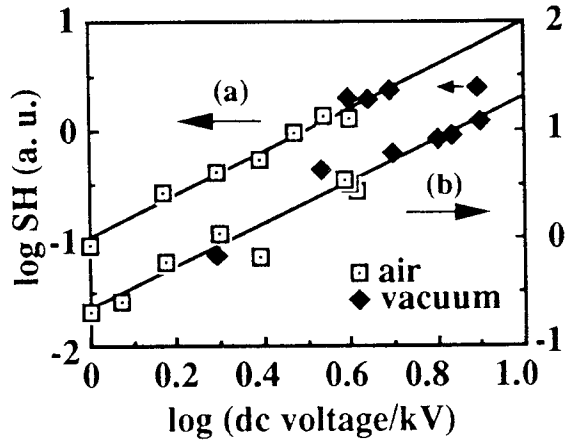

Fig. 5. log SHG versus log dc voltage for (a) the as-received Herasil 1 samples and for (b) repeatedly poled and annealed (for 1 h at 350 °C before poling) samples. Samples were poled at 280 °C. The poling time of the sample is optimum for a maximum SH signal for each dc voltage. Line (a) is fitted to as-received samples poled in air (the slope of the line is 1.98) Line (b) is fitted to all the repeatedly poled and annealed samples (the slope of the line is 1.92).

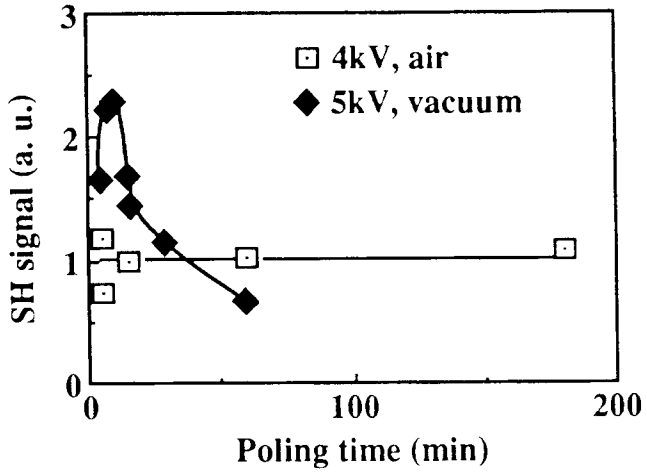

Fig. 6. SH signal versus poling time in air and vacuum for 1-mm-thick, repeatedly poled and annealed Herasil 1 samples poled at 280 °C.

an order of magnitude longer time for the signal to saturate (see Fig. 4)]. It should be noted that temperature hysteresis in the SH signal (which can be removed by annealing at a high temperature) had been observed earlier [34]. However, our results indicate that annealing does not restore the initial properties of the silica sample. The SH signal generated in the repeatedly poled and annealed samples is clearly proportional to the square of the applied dc voltage, without any sign of saturation, as in the similar dependence measured on the fresh samples (Fig. 5).

V. Quasi-Phase-Matched Second Harmonic Generation in Poled Optical Fibers

Because of their high nonlinear coefficients (more than one order of magnitude than for silica), lithium niobate (LN) [49] and KTP [50] potentially offer higher efficiencies for quasi-phase-matched optical frequency conversion in a waveguide geometry. For frequency conversion between 1.5 and 0.75 μm, however, silica has much lower dispersion than LN and KTP, thus much greater bandwidths available (more than one order of magnitude for the same device length) to nonlinear optical devices. This means that the lower value of nonlinearity can be compensated for by increasing the length of the device, thus achieving the same efficiency as for LN and KTP without altering the frequency stability. For example one can calculate that a perfectly periodically poled silica fiber with an effective nonlinear coefficient of 0.32 pm/V (starting nonlinear coefficient in the uniformly poled fiber of 1 pm/V), core diameter of 5.8 μm, numerical aperture of 0.09, length of 8 cm, can produce ~2 mW of blue light at 440 nm, when pumped with 100 mW. The acceptance bandwidth of such a device would be ~0.1 nm. These performances are comparable with those achieved in periodically poled LN and KTP waveguides [49], [50]. In addition, the group velocity mismatch (GVM) between pulses at different frequencies (which limits the effective interaction length) is in silica more than one order of magnitude less than in LN and KTP. This is promising for pulsed nonlinear optical processes.

Periodically patterned second order nonlinearities have been created in optical fibers by thermal poling in vacuo and cw quasi-phase-matched second harmonic (SH) generation to the blue has been demonstrated [40]. It should be pointed out that poling in vacuo gives much better on-off ratio in periodic structures than poling in air. In that work, the blue light at 430 nm was generated in the higher order mode $LP_{11}^{2\omega}$. In more recent work [48], we presented blue light generation at 440 nm, in the fundamental mode $LP_{01}^{2\omega}$, with an increase of a factor ~10 in the conversion efficiency in comparison with the previous results. The interaction with the higher order SH mode $LP_{11}^{2\omega}$ was suppressed by side-etching of the fiber surface.

The fiber used in the experiments was a D-shape fiber which had a Ge-doped silica core and a fused-silica cladding. The numerical aperture was 0.09, and the core and the outer diameters were 5.8 and 130 μm, respectively. The distance between the core region and the plane surface was 5 μm. The poling technique, based on continuous voltage of ~8 kV applied via aluminum electrodes at ~270 °C for ~10 min in vacuo, is the same as described above. For the experiments we prepared three samples. The first sample (A) was initially etched in a HF/H_2O (1:1) solution in order to reduce the core-surface distance from 5 to 1 μm and then uniformly poled over 10 mm. The second sample (B) was periodically poled over 6 mm with a pitch (including poled and nonpoled sections) of 28 μm. The third sample (C) was initially etched as sample A and then was periodically poled as sample B.

Before working on quasi-phase-matched second harmonic generation (QPM–SHG) with samples B and C we started evaluating the nonlinear coefficient in sample A via measurements of Maker's SH oscillations (see Fig. 8) for an interaction between fundamental modes at both fundamental and SH wavelengths (LP_{01}^{ω}–$LP_{01}^{2\omega}$) using a cw Ti:sapphire laser, tunable from 780 to 900 nm, as the fundamental source. The fact that the interaction was between fundamental modes was confirmed by imaging the near field pattern of the modes using a CCD camera connected to a TV monitor. We also checked that the polarizations of the output fundamental and

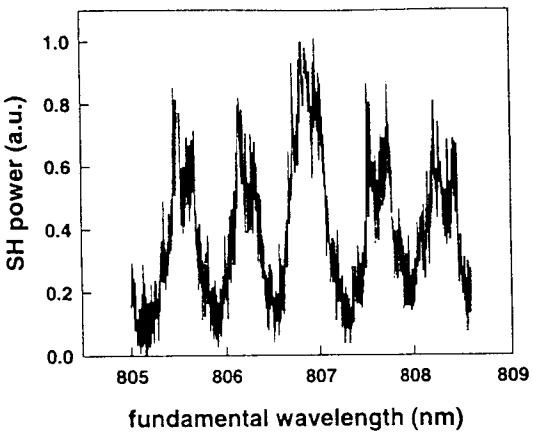

Fig. 7. SH power against fundamental wavelength for sample A, etched and uniformly poled.

SH beams were linear and perpendicular (as for the input fundamental) to the planar side of the D-shape fiber.

In a waveguide geometry [50], the SH power P_2 is given by

$$P_{2\omega} = \frac{8\omega^2 d^2}{n_{2\omega}^* n_\omega^{*2} \varepsilon_o c_o^3} \frac{P_\omega^2}{A_{\mathrm{OVL}}} \frac{1}{\Delta\beta^2} \sin^2\left(\frac{\Delta\beta L}{2}\right)\rho$$

where ω is the fundamental frequency, P_ω is the fundamental power, d is the nonlinear coefficient which includes the overlap between poled region and interacting modes, L is the device length, $n_{2\omega}^*$ and n_ω^* are the effective refractive indices at frequency 2ω and ω, respectively, ε_o the dielectric constant in vacuum, c_o the speed of light in vacuum, $A_{\mathrm{OVL}} = 1/I_{\mathrm{OVL}}^2$ is an equivalent area which depends on the overlap integral I_{OVL} between the interacting fields $\Delta\beta = \Delta\beta(\omega) = 2(\omega/c_o)(n_{2\omega}^* - n_\omega^*)$ is the wave-vector mismatch and ρ is an enhancement factor which takes account of the multimode nature of our fundamental source [50]. For $\Delta\beta L \gg 1$, this expression describes the Maker's oscillation, i.e., in our case, the nearly sinusoidal dependence of the SH power on the fundamental wavelength. One can easily confirm that the measured period of the Maker's SH modulation in Fig. 7 corresponds to a length of ~ 10 μm, indicating good agreement between theory and experimental results. Our calculation takes account of both material and modal dispersion. The material dispersion is described by a Sellmeier equation (dependence of refractive index on wavelength) derived from the best fit of numerical data provided by the manufacturer. For example in our fiber and for a $\mathrm{LP}_{01}^{\omega}$–$\mathrm{LP}_{01}^{2\omega}$ interaction the contributions to $\Delta\beta$ at $\lambda = 805$ nm due to material and waveguide dispersion are ~ 0.26 $\mu\mathrm{m}^{-1}$ and ~ 0.016 $\mu\mathrm{m}^{-1}$, respectively. The measured SH power was ~ 100 pW, corresponding to a fundamental power of ~ 70 mW. From these powers, assuming $\rho = 2$, we evaluated $d \sim 0.7$ pm/V. This value of $d\,[\sim \chi^{(2)}/2]$ corresponds to a second-order nonlinear susceptibility $\chi^{(2)}$ of ~ 1.4 pm/V, which is about three times higher than in our experiments with side polished fibers. This increase can be explained by optimized parameters of the fiber and poling.

After these preliminary SH measurements to determine the nonlinear coefficient we optically assessed samples B and C via QPM–SHG to the blue. Figs. 8 and 9 show the SH power against fundamental wavelength for samples B and C,

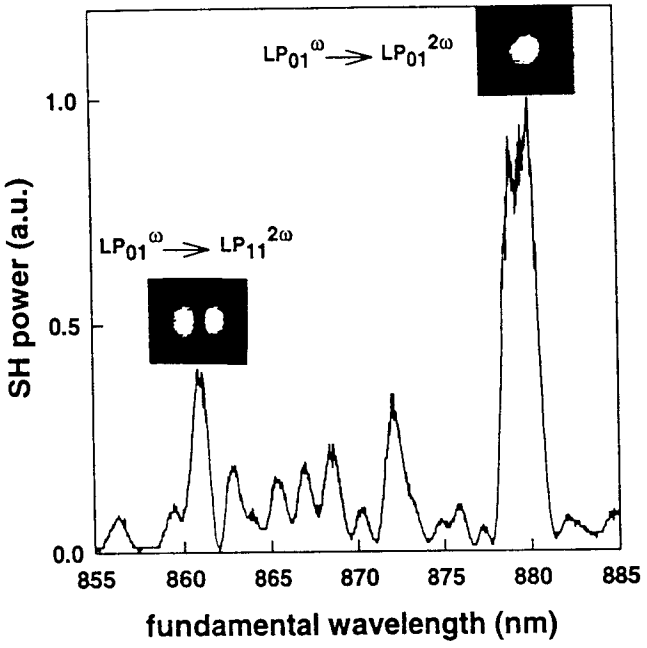

Fig. 8. SH power against fundamental wavelength for sample B, periodically poled. The maximum SH power is 2 nW.

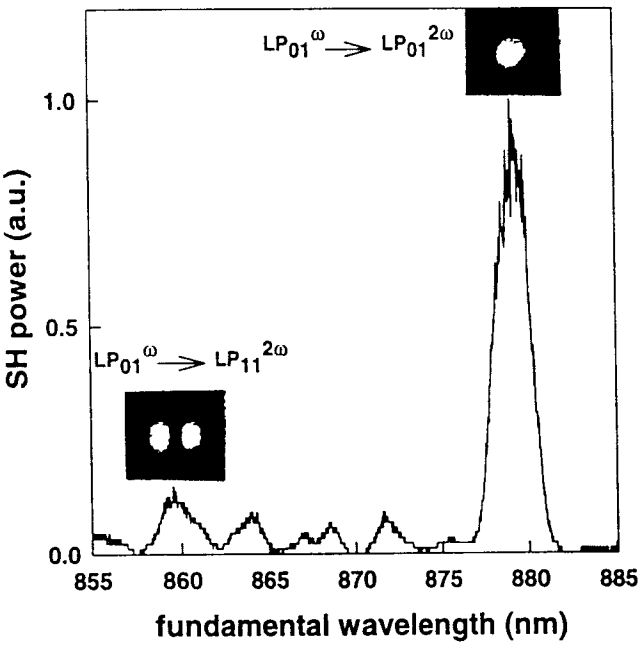

Fig. 9. SH power against fundamental wavelength for sample C, etched and periodically poled. The maximum SH power is 10 nW.

indicating for both samples the presence of interaction with both the fundamental SH mode $\mathrm{LP}_{01}^{2\omega}$ and the higher order SH mode $\mathrm{LP}_{11}^{2\omega}$ at a fundamental wavelength of ~ 880 and ~ 860 nm, respectively. These wavelengths for QPM–SHG are in good agreement with the theoretical predictions of ~ 873 and ~ 851 nm.

The fact that the interaction ($\mathrm{LP}_{01}^{\omega}$–$\mathrm{LP}_{11}^{2\omega}$) between the fundamental mode $\mathrm{LP}_{01}^{\omega}$ and the odd higher order SH mode $\mathrm{LP}_{11}^{2\omega}$ is allowed indicates that the poled region is not centered with respect to the core. If it were centered the overlap integral between the interacting fields and the poled region would be

zero because of modal symmetry. In sample B, the interaction with the higher order SH mode $LP_{11}^{2\omega}$ is stronger than in fiber C. This is probably associated with the increase of the core-surface distance from 1 to 5 μm. This increase is believed to reduce the loss for higher order modes and to move the poled region out of the center of the core. In fact the poled region, located a few microns under the surface, and the core have approximately the same size and it is not surprising that they are more off-center with respect to each other in sample B than in sample C.

The presence of strong side-peaks in Figs. 8 and 9 is probably an indication of the fact that the grating is not uniform along the direction of propagation. This was confirmed by launching the beam from a 1.064 μm Q-switched and mode locked Nd:YAG laser transversely to the fiber C. The beam was focused in the grating region of the fiber and the corresponding SH near field was imaged by a CCD camera connected to a TV monitor. Fig. 10 shows clearly the presence of regions where the grating is almost absent [see Fig. 10(a)] together with regions where an evident periodic modulation of the nonlinearity is present [see Fig. 10(b)]. We believe that the absence of the grating is mainly due to spreading of the poled regions. This is consistent with the fact that the regions where there is no evidence of grating structure, provided a uniform SH signal rather than absence of SH signal [see Fig. 10(a)]. Note that Fig. 10(a) and (b) are on different scales. The side peaks (see Figs. 8 and 9) are stronger in the case of sample B than of sample C. A possible explanation is that the location of the poled region with respect to the core varies longitudinally along the fiber, thus making the overlap integral longitudinally change. This is more likely to occur in fiber B than in fiber C and is equivalent to a grating longitudinally non uniform.

The maximum SH power detected for sample B was ~2 nW, corresponding to a fundamental power in the fiber of ~230 mW. For sample C these values were ~10 nW and ~230 mW, respectively. From the above expression for the SH power one can estimate that the effective nonlinear coefficient d_{eff} (average over the whole 6-mm-grating length) is >50 times smaller than the expected value of 0.22 pm/V ($= d/\pi$) for a perfect grating with an amplitude d of 0.7 pm/V (which is the nonlinear coefficient measured in the uniformly poled sample A). We believe that this degradation is mainly due to the aforesaid nonuniformity of the grating although it is not excluded that the nonoptimization of the overlap integral plays a role in reducing the efficiency. In fact, we observed during the experiment relative to Fig. 10 that the grating structure is limited to small regions, giving an equivalent total interaction length much less than the expected 6 mm. The fact that some regions were modulated and others were not is probably due to the use of a periodic anode which was not uniformly pressed on the fiber during poling (the starting fiber itself and the etching could also be not completely uniform).

VI. Pockels Effect in Thermally Poled Optical Fibers

In this section, we discuss our measurements of the Pockels effect in optical fibers thermally poled in vacuum [39].

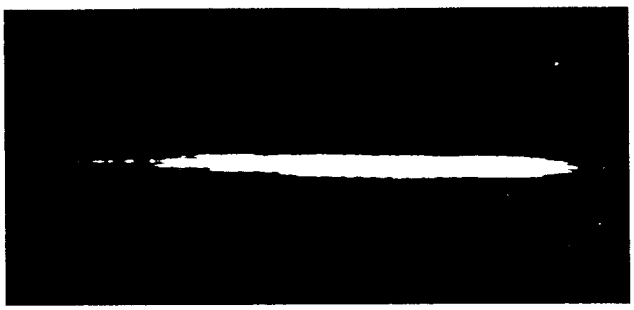

28 μm

(a)

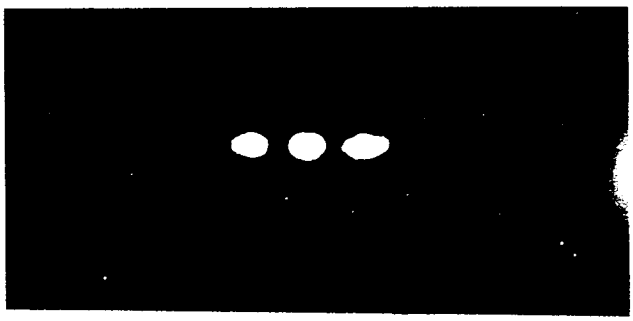

28 μm

(b)

Fig. 10. Near field second-harmonic patterns, imaged by launching the fundamental 1.064-m beam transversely to the fiber. There is evidence of regions where (a) the modulation of the nonlinearity is extremely weak, due to spreading of the poled sections and (b) particularly evident. Note that figures (a) and (b) are on different scales.

Ge-doped fiber with fused silica cladding, numerical aperture 0.09, core and outer diameter 6 and 90 μm was used in experiment. The LP_{11} cutoff wavelength of the fiber was 740 nm. Regions about 8 mm long were side-polished to within 1 μm of the core using a wheel polishing technique. The fibers were poled at 9 kV applied voltage, 280 °C temperature for 15 min in an evacuated chamber at 1.2×10^{-5} mbar.

A Mach–Zehnder fiber optic interferometer was used for measurement of the electrooptic phase shifts (Fig. 11). Pieces of fiber about 40 cm long with 8 cm long poled regions in the middle were fusion-spliced into one arm of a Mach–Zehnder interferometer made from fibers single mode at 830 nm. A semiconductor laser operating at 830 nm was used as the light source. The poled fiber was fixed to a supporting plastic plate with one electrode underneath the poled region and a second electrode 6 mm long pressed to the polished region. A signal from an ac voltage generator with frequency 0–50 kHz and amplitude 0–150 V was applied to the electrodes. The difference signal from the output of two silicon detectors

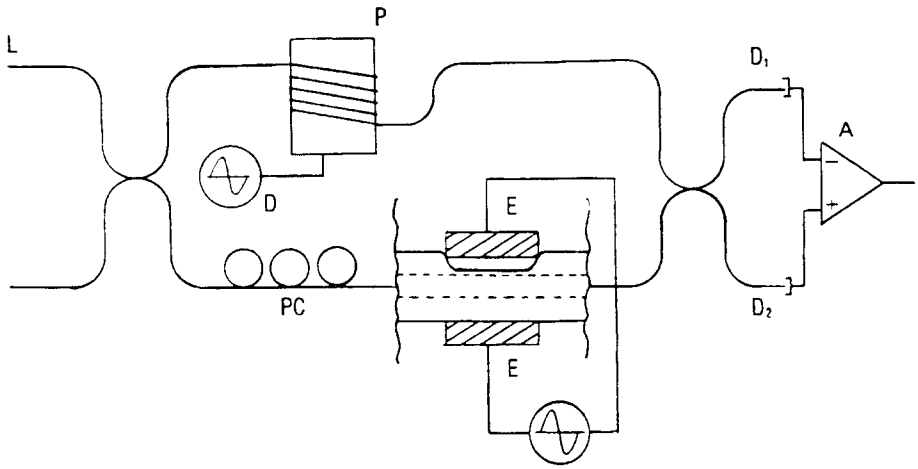

Fig. 11. Mach–Zehnder fiber-optic interferometer with poled fiber. P: piezoelectric tube, PC: polarization controller, D: dither waveform, $D_{1,2}$: detectors, A: difference amplifier, L: laser, E: electrodes.

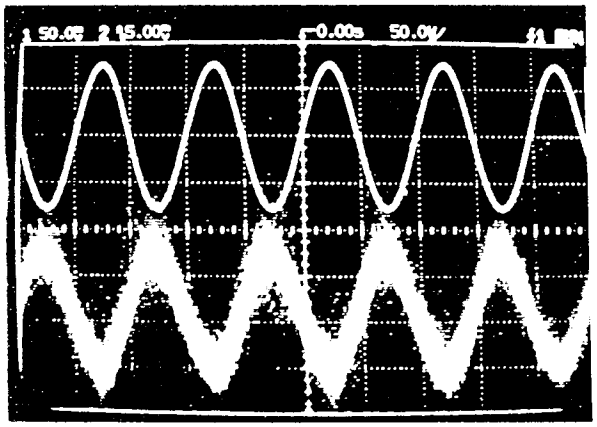

Fig. 12. Applied ac voltage (a) and output signal of Pockels modulation from silicon detectors (b) in single-mode fiber. Peak-to-peak voltage is 150 V.

was monitored using an oscilloscope. The operating point of the interferometer was locked by means of a control system for signal stabilization. To this end the difference signal was applied to the input of an integrator and the amplified output of the integrator used to drive a piezoelectric modulator placed in one arm of the interferometer.

First of all, for careful measurements of the relatively low signal from the Pockels effect, it was necessary to eliminate the strong signal from fiber vibrations caused by electrostatic forces acting on the poled fiber [28]. We succeeded in doing this by proper fixation of the fiber and applying uniform pressure on the poled region. The output signal from the silicon detectors—we believe, due to Pockels effect in the poled fiber—is shown together with the applied ac voltage in Fig. 12. The output signal was almost uniform in the measured frequency range up to 50 kHz and showed no evidence of acoustic resonances.

We have measured phase shifts of about 15 mrad for a 50 μm gap in the single mode fiber at an applied voltage of 75 V and an electrode length of 6 mm. These measurements give a value of effective electrooptic coefficient ($r^* = r\eta = \Delta\phi\lambda D\pi^{-1}n^{-3}V^{-1}L^{-1}$, r—electrooptic coefficient, $\Delta\phi$—phase shift, λ—wavelength, D—gap between electrodes, V—applied voltage, L—lectrode length, η—overlap factor between poled region and fiber mode) of about 0.15 pm/V. Assuming the value of electrooptic coefficient to be 0.3 pm/V [27], the value of the overlap factor is estimated to be about 0.5.

Electrooptic coefficients as high as 0.3 pm/V were also measured in thermally poled commercial D-shaped fibers [42]. D-shaped fiber was glued to an Si wafer using a thin polyimide layer. The fiber was also covered with polyimide layers to avoid breakdown and allow volume manufacturing of travelling wave modulators. It is interesting that the optimum poling time of about 10 min was observed in this work. This observation is similar to our observation of the optimum poling time in vacuum poled fibers and gives additional confirmation that some species from the air, e.g., hydrogen ions, are responsible for the saturation of the SH signal during poling in air.

Recently, Fujiwara *et al.* have reported an electrooptic coefficient of about ~6 pm/V in germanosilicate fiber poled via internal electrodes in the presence of UV light of wavelength 193 nm from an ArF excimer laser [41]. Although, UV excitation was used, it seems this is not the major factor responsible for the high value measured. Indeed, even without UV excitation the measured coefficient is comparable to the one obtained in thermally poled fibers, and two to three orders of magnitude higher than in prior similar experiments made in fibers with internal electrodes [9]. Further experiments are needed to clarify the underlying mechanism.

VII. Conclusions

A better understanding of the physical mechanisms behind glass poling may lead to even higher values of nonlinearity and thence to the development of a range of new fiber devices. Potentially important areas of applications of poled glass fibers include also: 1) enhancement of nonlinear refractive index (n_2) of silica as a result of cascading of the second-order nonlinear processes (100 times increase in effective n_2 can be achieved), 2) generation of photon pairs by parametric down-conversion for all-fiber quantum cryptography and noiseless parametric

amplification, 3) frequency conversion of short and soliton pulses in fibers using the advantage of low dispersion of silica glass (the group velocity mismatch at 860 nm is about 130 fs/mm in silica compared to 1.8 ps/mm in lithium niobate), and 4) excellent UV transparency of silica glass is another advantage of this material which may found important applications in generation of ultrashort UV pulses by frequency doubling needed for temporal domain photoluminescence studies and optical storage.

REFERENCES

[1] U. Österberg and W. Margulis, "Dye laser pumped by Nd:YAG laser pulses frequency doubled in glass optical fiber," *Opt. Lett.*, vol. 11, pp. 516–518, 1986.

[2] R. H. Stolen and H. W. K. Tom, "Self-organized harmonic generation in optical fibers," *Opt. Lett.*, vol. 12, pp. 585–587, 1987.

[3] N. B. Baranova and B. Ya. Zeldovich, "Extention of holography to multi-wavelength field," *JETP Lett.*, vol. 46, pp. 716–718, 1987.

[4] M. C. Farries, P. St. J. Russell, M. E. Fermann, and D. N. Payne, "Second harmonic generation in an optical fiber by self-written $\chi^{(2)}$ grating," *Electron. Lett.*, vol. 23, pp. 322–324, 1987.

[5] E. M. Dianov, P. G. Kazansky, and D. Yu. Stepanov, "Problem of the photoinduced second harmonic generation," *Sov. J. Quantum. Electron.*, vol. 19, pp. 575–576, 1989.

[6] E. M. Dianov, P. G. Kazansky, D. S. Starodubov, and D. Yu. Stepanov "Photoinduced second harmonic generation: Observation of charge separation due to the photovoltaic effect," *Sov. Lightwave Commun.*, vol. 3, pp. 247–250, 1991.

[7] F. Ouellette, K. Hill, and D. C. Johnson, "Enhancement of second-harmonic generation in optical fibers by hydrogen and heat treatment," *Appl. Phys. Lett.*, vol. 54, pp. 1086–1088, 1989.

[8] R. Kashyap, "Phase-matched periodic electric-field-induced second-harmonic generation in optical fibers," *J. Opt. Soc. Amer. B*, vol. 6, pp. 313–328, 1989.

[9] L. Li and D. N. Payne, "Permanently-induced linear electro-optic effect in silica optical fibers," in *Proc. Dig. Conf. Integrated and Guided Wave Optics*. Optic. Soc. Amer., Washington, DC, 1989, paper TuAA2-1.

[10] V. Mizrahi, Y. Hibino, and G. Stegeman, "Polarization study of photoinduced second-harmonic generation in glass optical fibers," *Opt. Commun.*, vol. 78, pp. 283–288, 1990.

[11] A. Kamal, D. A. Weinberger, and W. H. Weber,"Spatially resolved Raman study of self-organized $\chi^{(2)}$ gratings in optical fibers," *Opt. Lett.*, vol. 15, pp. 613–615, 1990.

[12] M. D. Selker and N. M. Lawandy, "Observation of seeded second-harmonic generation in bulk germanosilicate fiber preform," *Opt. Commun.*, vol. 77, pp. 339–344, 1991.

[13] D. Anderson, V. Mizrahi, and J. E. Sipe, "Model for second-harmonic generation in glass optical fibers based on asymmetric photoelectron emission from defect sites," *Opt. Lett.*, vol. 16, pp. 796–798, 1991.

[14] F. Charra, F. Devaux, J. M. Nunzi, and P. Raimond, "Picosecond light-induced noncentrosymmetry in dye solution," *Phys. Rev. Lett.*, vol. 68, pp. 2440–2443, 1992.

[15] V. Dominic and J. Feinberg, "Growth rate of second-harmonic generation in glass," *Opt. Lett.*, vol. 17, pp. 1761–1763, 1992.

[16] D. M. Krol, D. J. DiGiovanni, W. Pleibel, and R. H. Stolen, "Observation of resonant enhancement of photoinduced second-harmonic generation in Tm-doped aluminosilicate glass fibers," *Opt. Lett.*, vol. 18, pp. 1220–1222, 1993.

[17] W. Margulis, F. Laurell, and B. Lesche, "Imaging the nonlinear grating in frequency-doubling glass fibers," *Nature*, vol. 348, pp. 699–701, 1995.

[18] R. A. Myers, N. Mukherjee, and S. R. J. Brueck, "Large second-order nonlinearities in poled fused silica," *Opt. Lett.*, vol. 16, pp. 1732–1734, 1991.

[19] A. Okada, K. Ishii, K. Mito, and K. Sasaki, "Second-harmonic generation in novel corona poled glass waveguides," *Appl. Phys. Lett.*, vol. 60, pp. 2853–2855, 1992.

[20] P. G. Kazansky, A. Kamal, and P. St. J. Russell, "High second-order nonlinearities induced in lead silicate glass by electro-beam irradiation," *Opt. Lett.*, vol. 18, pp. 693–695, 1993.

[21] K. Tanaka, K. Kashima, K. Hirao, N. Soga, A. Mito, and H. Nasu, "Second-harmonic generation on poled tellurite glasses," *Japan J. Appl. Phys.*, vol. 32, pp. 843–844, 1993.

[22] P. G. Kazansky, A. Kamal, and P. St. J. Russell, "Erasure of thermally poled second-order nonlinearity in fused silica by electron implantation," *Opt. Lett.*, vol. 18, pp. 1141–1142, 1993.

[23] A. C. Liu, M. J. F Digonnet, and G. S. Kino, "Electro-optic phase modulation in silica channel waveguide," *Opt. Lett.*, vol. 19, pp. 466–448, 1994.

[24] N. Mukherjee, R. A. Myers, and S. R. J. Brueck, "Dynamics of second-harmonic generation in fused silica," *J. Opt. Soc. Amer. B*, vol. 11, pp. 665–669, 1994.

[25] P. G. Kazansky, L. Dong, and P. St. J. Russell, "High second-order nonlinearities in poled silicate fibers," *Opt. Lett.*, vol. 19, pp. 701–703, 1994.

[26] ——, "Vacuum poling: An improved technique for effective thermal poling of silica glass and gemanosilicate optical fibers," *Electron. Lett.*, vol. 30, pp. 1345–1347, 1994.

[27] X.-C. Long, R. A. Myers, and S. R. J. Brueck, "The electro-optic effect in poled amorphous silica," *Opt. Lett.*, vol. 19, pp. 1819–1821, 1994.

[28] P. G. Kazansky, P. St. J. Russell, and C. N. Pannell, "Optical fiber electrets: Observation of electro-acousto-optic transduction," *Electron. Lett.*, vol. 30, pp. 1436–1347, 1994.

[29] X.-C. Long, R. A. Myers, and S. R. J. Brueck, "Measurement of linear electro-optic effect in temperature/electric-field poled optical fibers," *Electron. Lett.*, vol. 30, pp. 2162–2163, 1994.

[30] R. Kashyap, G. J. Veldhuis, D. C. Rogers, and P. F. McKee, "Phase-matched second-harmonic generation by periodic poling of fused silica," *Appl. Phys. Lett.*, vol. 64, pp. 1332–1334, 1994.

[31] P. G. Kazansky and P. St. J. Russell, "Thermally poled glass: Frozen-in electric field or oriented dipoles," *Opt. Commun.*, vol. 101, pp. 611–614, 1994.

[32] R. A. Myers, S. R. Brueck, and R. P. Tumminelli, "Stable second-order nonlinearity in SiO_2-based waveguides on Si using temperature/electric field poling," *Proc. SPIE*, vol. 2289, pp. 158–166, 1994.

[33] R. A. Myers, X.-C. Long, S. R. J. Brueck, and R. P. Tumminel "The effect of hydrogen loading on temperature/electric-field poling SiO_2-based thin films," *Electron. Lett.*, vol. 32, pp. 1604–1606, 1995.

[34] R. A. Myers, X.-C. Long, and S. R. J. Brueck, "Recent advances in the second-order nonlinear optical properties of amorphous silica materials," *Proc. SPIE*, vol. 2289, pp. 98–109, 1994.

[35] H. Nasu, H. Okamoto, K. Kurachi, J. Matsuoka, K. Kamiya, A. Mito, and H. Hosono, "Second-harmonic generation from electrically poled SiO_2 glass: Effects of OH concentration, defects, and poling conditions," *J. Opt. Soc. Amer. B*, vol. 12, pp. 644–649, 1995.

[36] K. Tanaka, K. Kashima, K. Hirao, N. Soga, S. Yamagata, A. Mito, and H. Nasu, "Effect of γ-irradiation on optical second harmonic intensity of electrically poled silica glass," *Japan J. Appl. Phys.*, vol. 34, 173–17 1995; "Highly efficient optical second harmonic generation in po Ti-doped silica glasses," *Japan J. Appl. Phys.*, vol. 43, pp. 175–17 1995.

[37] L. J. Henry, A. D. DeVilbiss, and T. E. Tsai, "Effect of annealing on the level of second harmonic generation and defect sites achieved in poled fused silica," *J. Opt. Soc. Amer. B*, vol. 12, pp. 2037–2047, 1995.

[38] Y. Zhao, G. Town, and M. Sceats, "$\chi^{(3)}$ effects on the nonlinear phase shifts from SHG in optical fibers," *Opt. Commun.*, vol. 115, pp. 129–133, 1995.

[39] P. G. Kazansky, P. St. J. Russell, L. Dong, and C. N. Pannell, "Pockels effect in thermally poled silica optical fibers," *Electron. Lett.*, vol. 3 pp. 62–63, 1995.

[40] P. G. Kazansky, V. Pruneri, and P. St. J. Russell, "Blue-light generati by quasiphase-matched frequency doubling in thermally poled optic fibers," *Opt. Lett.*, vol. 20, pp. 843–845, 1995.

[41] T. Fujiwara, D. Wong, Y. Zhao, S. Fleming, S. Poole, and M. Sceats, "Electro-optic modulation in germanosilicate fiber with UV-excited poling," *Electron. Lett.*, vol. 31, pp. 573–575, 1995.

[42] X.-C. Long, R. A. Myers, and S. R. J. Brueck, "A poled electro-optic fiber," *IEEE Photon. Technol. Lett.*, vol. 8, pp. 227–229, 1996.

[43] M. Abe, T. Kitagawa, K. Hattori, A. Himeno, and Y. Ohmori, "Electro-optic switch constructed with a poled silica-based waveguide on Si substrate," *Electron. Lett.*, vol. 30, pp. 893–894, 1996.

[44] P. G. Kazansky, A. R. Smith, P. St. J. Russell, G. M. Yang, and M. Sessler, "Thermally poled silica glass: Laser induced pressure pu probe of charge distribution," *Appl. Phys. Lett.*, vol. 68, pp. 269–2 1996.

[45] S. Horinouchi, H.Imai, G. J. Zhang, K. Mito, and K. Sasaki, "Optical quadratic nonlinearity in multilayer corona-poled glass films," *Appl. Phys. Lett.*, vol. 68, pp. 3552–3554, 1996.

[46] L. J. Henry, B. V. McGrath, T. G. Alley, and J. J. Kester, "Optical nonlinearity in fused silica by proton implantation," *J. Opt. Soc. Am. B*, vol. 13, pp. 827–836, 1996.

[47] H. Takebe, P. G. Kazansky, P. St. J. Russell, and K. Morinaga, "Effect of poling conditions on second-harmonic generation in fused silica"

Opt. Lett., vol. 20, pp. 468–470, 1996.
[48] V. Pruneri and P. G. Kazansky, "Electric-field thermally poled optical fibers for quasiphase-matched second harmonic generation," *IEEE Photon. Technol. Lett.*, vol. 6, pp. 185–187, 1997.
[49] M. Yamada, N. Nada, M. Saitoh, and K. Watanabe, "First-order quasiphase-matched $LiNbO_3$ waveguide periodically poled by applying an external field for efficient blue second-harmonic generation," *Appl. Phys. Lett.*, vol. 62, pp. 435–436, 1993.
[50] Q. Chen and W. P. Risk, "High efficiency quasiphase-matched frequency doubling waveguides in $KtiOPO_4$ fabricated by electric field poling," *Electron. Lett.*, vol. 32, pp. 107–108, 1996.
[51] S. Helmfrid and G. Arvidsson, "Second-harmonic generation in quasiphase-matching waveguides with a multimode pump," *J. Opt. Soc. Amer. B*, vol. 8, pp. 2326–2330, 1991.

Peter G. Kazansky was born in Moscow, U.S.S.R., on November 17, 1956. He graduated from Moscow State University in 1979 and received the Ph.D. degree in physics from the General Physics Institute, Moscow, in 1985.

He has more than 18 years experience pertinent to quantum electronics, fiber, and integrated optics. For the pioneering work on "Circular photogalvanic effect in crystals" he was awarded the Leninskii Komsomol Prize in 1989. From 1989 to 1993, he led a group in the General Physics Institute which unraveled the mystery of a new nonlinear optical phenomenon-photo-induced frequency doubling in centrosymmetric media. He was awarded the title "Senior Research Fellow in Physical Electronics" in 1992. In 1993, he was awarded a Royal Society Fellowship at the Optoelectronics Research Centre, University of Southampton. Currently, he is a Group Leader at the ORC working in advanced nonlinear optical materials.

Dr. Kazansky is a member of the Optical Society of America and the American Physical Society.

Philip St. J. Russell, for a biography, see this issue, p. 1262.

Hiromichi Takebe was born in Saga, Japan, on February 13, 1963. He received the B.E. degree in metallurgy from Kyushu University, Fukuoka, Japan, in 1986. He received the Master and Doctor degrees of Engineering in materials sciences from Kyushu University, Japan, in 1988 and 1991, respectively.

He was Assistant Professor from 1991 to 1993 and is now an Associate Professor, Department of Materials Science and Technology, Graduate School of Engineering Sciences, Kyushu University. He also joined Optoelectronics Research Centre, University of Southampton, Southampton, UK, in 1997 as a Visiting Research Fellow. He published more than 50 scientific papers.

Dr. Takebe is a member of the Japan Society of Applied Physics, American Ceramic Society, Ceramic Society of Japan, the Mining and Materials Processing Institute of Japan, and Japan Institute of Metal. He received the award for young scientists in the Mining and Materials Processing Institute of Japan in 1996.